# The underlying event and the total cross section from Tevatron to the LHC



JHEP01(2009)065

(http://iopscience.iop.org/1126-6708/2009/01/065)

Published by IOP Publishing for SISSA
Received: *July 4, 2008*
Revised: *November 27, 2008*
Accepted: *January 7, 2009*
Published: *January 23, 2009*

# The underlying event and the total cross section from Tevatron to the LHC

**Manuel Bähr,**[ab] **Jonathan M. Butterworth**[b] **and Michael H. Seymour**[cd]

[a] *Institut für Theoretische Physik, Universität Karlsruhe, 76128 Karlsruhe, Germany*
[b] *High Energy Physics Group, Dept. of Physics and Astronomy Mathematical and Physical Sciences, University College, London Gower Street, London, WC1E 6BT, U.K.*
[c] *School of Physics and Astronomy, University of Manchester, Oxford Road, Manchester, M13 9PL, U.K.*
[d] *Physics Department, CERN, CH-1211 Geneva 23, Switzerland*
*E-mail:* mb@particle.uni-karlsruhe.de, J.Butterworth@ucl.ac.uk., Michael.Seymour@cern.ch

Abstract: Multiple partonic interactions are widely used to simulate the hadronic final state in high energy hadronic collisions, and successfully describe many features of the data. It is important to make maximum use of the available physical constraints on such models, particularly given the large extrapolation from current high energy data to LHC energies. In eikonal models, the rate of multiparton interactions is coupled to the energy dependence of the total cross section. Using a Monte Carlo implementation of such a model, we study the connection between the total cross section, the jet cross section, and the underlying event. By imposing internal consistency on the model and comparing to current data we constrain the allowed range of its parameters. We show that measurements of the total proton-proton cross-section at the LHC are likely to break this internal consistency, and thus to require an extension of the model. Likely such extensions are that hard scatters probe a denser matter distribution inside the proton in impact parameter space than soft scatters, a conclusion also supported by Tevatron data on double-parton scattering, and/or that the basic parameters of the model are energy dependent.

Keywords: Jets, Phenomenological Models, Hadronic Colliders, QCD.



JHEP01(2009)065

## Contents



## 1. Introduction

Hadron-hadron collision events at high energies often contain high transverse energy jets, which in QCD arise from gluon or quark (generically, parton) scattering followed by QCD radiation and hadronization. This model is generally taken to be realistic above some minimum transverse momentum scale, $p_t^{\min}$. The contribution of these events to the total cross section rises with hadron-hadron centre-of-mass energy, $s$, since the minimum value of the $x$ probed is given by $4(p_t^{\min})^2/s$, and the parton densities rise strongly for $x < 10^{-2}$ or so [1, 2].

One reason that this rising contribution to the cross section is of interest is that while perturbative QCD cannot predict total hadronic cross sections (since in many events no hard perturbative scale is present), rising hadronic cross sections are a feature also seen in successful non-perturbative approaches [3, 4], the behaviour of which must presumably emerge from the QCD Lagrangian in some manner. Thus by comparing the behaviour of the hard contribution to the cross section to the behaviour expected from fits to the total cross section, it may be possible to learn something about the connection between these approaches and about hadronic cross sections in general.

The connection between the hard partonic cross section and the total cross section is not one-to-one, however. There are certainly hadronic scatters in which no hard jets are produced, and some non-perturbative scattering process must be added to the perturbative jet contribution to model the total cross section. In addition, at the high parton densities



JHEP01(2009)065

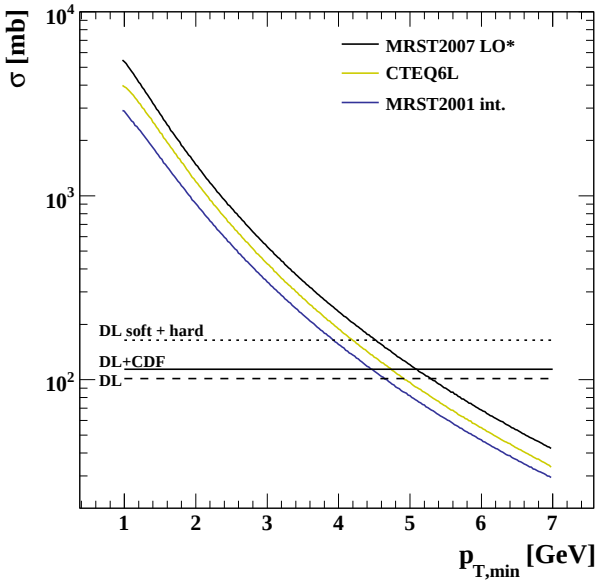


**Figure 1:** The inclusive hard cross section for three different proton PDFs, compared to various extrapolations of the non-perturbative fits to the total $pp$ cross section at 14 TeV centre-of-mass energy.

probed at recent, current and future colliders, simple assumptions lead to the conclusion that the probability of multiple partonic scatters in a single hadron-hadron collision is significant. In fact, figure 1 shows that for $p_t^{\min}$ values below about 5 GeV, the total "hard" cross section calculated assuming one parton-parton scatter per proton-proton collision *exceeds the total cross section* as extrapolated using the non-perturbative fits, at LHC energies. This strongly implies that the average number of partonic scatters in an inelastic collision must be greater than one.

Introducing the possibility of such multiparton interactions also seems to be required in order to describe the hadronic final state [5 – 7]. In general, softer additional scatters occurring in a high-$p_t$ event manifest themselves as additional particles and energy-flow, the so-called "underlying event".

In this paper we examine the predictions of the model that was discussed, for example in [8], and implemented in [9 – 12] including the possibility of soft scatters. We explore the consistency constraints that would be imposed by comparing a given value of the total cross section to the predicted jet cross section, and attempt to identify allowed regions of parameter space within which the model must lie if it is to be consistent with the measured cross section at the LHC. We also discuss ways in which energy dependencies in the parameters could arise, and their impact upon these constraints. The studies are all carried out using the new implementation in Herwig++ [11, 12]; however, they are also relevant to the fortran implementation Jimmy [9], if the same hard cross section is used.

## 2. Total and elastic cross section parameterizations

Throughout this paper we will exploit the connection that can be established between



JHEP01(2009)065

the eikonal model of refs. [9 – 11] and the total cross section. To give a reasonable range of expectations for the latter, we use the successful parameterization of Donnachie and Landshoff [3, 4]. We will use three different variations;

1. The *standard* parameterization from [3] with the following behaviour at high energies:

$$\sigma_{\rm tot} \sim 21.7 \text{ mb} \cdot \left(\frac{s}{\text{GeV}^2}\right)^{0.0808} \rightarrow \sigma_{\rm tot}(14 \text{ TeV}) = 101.5 \text{ mb}\,. \tag{2.1}$$

2. Using the same energy dependence but normalizing it to the measurement [13] by CDF:

$$\sigma_{\rm tot} \sim 24.36 \text{ mb} \cdot \left(\frac{s}{\text{GeV}^2}\right)^{0.0808} \rightarrow \sigma_{\rm tot}(14 \text{ TeV}) = 114.0 \text{ mb}\,. \tag{2.2}$$

3. Using the most recent fit [4], which takes the contributions from both hard and soft Pomerons into account:

$$\sigma_{\rm tot} \sim 24.22 \text{ mb} \cdot \left(\frac{s}{\text{GeV}^2}\right)^{0.0667} + 0.0139 \text{ mb} \cdot \left(\frac{s}{\text{GeV}^2}\right)^{0.452} \rightarrow \sigma_{\rm tot}(14 \text{ TeV}) = 164.4 \text{ mb}\,. \tag{2.3}$$

Other parameterizations and models for the total cross section exist [14, 15], but their predictions for the total cross section at 14 TeV generally lie within the range covered by these three[1]. As will be seen, the range is wide, and early measurements of the total cross section at the LHC can be expected to have a big impact [18].

We will also find it useful to compare our model with the elastic slope parameter, $B$, defined in terms of the differential elastic scattering cross section, $\mathrm{d}\sigma/\mathrm{d}t$, as

$$B = B(s, t=0) = \left[\frac{\mathrm{d}}{\mathrm{d}t}\left(\ln\frac{\mathrm{d}\sigma}{\mathrm{d}t}\right)\right]_{t=0}. \tag{2.4}$$

In the Donnachie-Landshoff parameterization, this is given by:

$$B = 2\alpha' \ln\frac{s}{s_0} + B_0 \tag{2.5}$$

with $\alpha' = 0.25$ GeV$^{-2}$. Together with the CDF data [19], this implies

$$B = \left(\ln\frac{\sqrt{s}}{1800 \text{ GeV}} + (17 \pm 0.25)\right) \text{ GeV}^{-2} = \left(\ln\frac{\sqrt{s}}{14 \text{ TeV}} + (19 \pm 0.25)\right) \text{ GeV}^{-2}. \tag{2.6}$$

The most recent fit [4] has the same value for $\alpha'$ and hence $B$, while those of [14, 15] are a little higher: 20–22 GeV$^{-2}$. We therefore use the CDF value for the Tevatron energy and the range 19–22 GeV$^{-2}$ to represent the range of possible measurements from the LHC.

[1] The most recent models of [16, 17] predict $\sigma_{\rm tot}(14 \text{ TeV}) \simeq 90$ mb, which is 10 % below the smallest expectation we use. Since the difference this introduces is similar to the one between our first and second parameterization it can easily be estimated by the reader.



JHEP01(2009)065

## 3. Eikonal model

The scattering amplitude $\mathcal{A}(s,t)$ can be expressed as the Fourier transform of the elastic scattering amplitude $a(\mathbf{b},s)$ in impact parameter space as

$$\mathcal{A}(s,t) = 4s \int \mathrm{d}^2b \;\; a(\mathbf{b},s)\, e^{i\mathbf{q}\cdot\mathbf{b}} \;, \tag{3.1}$$

where $\mathbf{q}$ is the transverse momentum transfer vector, with, in the high energy limit, $\mathbf{q}^2 = -t$. In this limit, $a(\mathbf{b},s)$ can be assumed to be purely imaginary and therefore be expressed in terms of a real eikonal function $\chi(\mathbf{b},s)$, as

$$a(\mathbf{b},s) = \frac{1}{2i}\left[\, e^{-\chi(\mathbf{b},s)} \;-1\right] . \tag{3.2}$$

Using (3.1) and (3.2) the total cross section for $pp \to X$ can be expressed as

$$\begin{aligned} \sigma_{\mathrm{tot}} &= \frac{1}{s}\Im\left\{\mathcal{A}(s,t=0)\right\} \\ &= 2\int \mathrm{d}^2b \;\; \left[1 - \; e^{-\chi(\mathbf{b},s)}\,\right] . \end{aligned} \tag{3.3}$$

The elastic cross section is then

$$\begin{aligned} \sigma_{\mathrm{el}} &= 4\int \mathrm{d}^2b \;\; |a(\mathbf{b},s)|^2 \\ &= \int \mathrm{d}^2b \;\; \left|1 - \; e^{-\chi(\mathbf{b},s)}\,\right|^2 . \end{aligned} \tag{3.4}$$

The inelastic cross section thereby reads

$$\begin{aligned} \sigma_{\mathrm{inel}} &= \sigma_{\mathrm{tot}} - \sigma_{\mathrm{el}} \\ &= \int \mathrm{d}^2b \;\; \left[1 - \; e^{-2\chi(\mathbf{b},s)}\,\right] . \end{aligned} \tag{3.5}$$

The elastic slope parameter at zero momentum transfer is also calculable within this framework and yields [20]

$$B = \frac{1}{\sigma_{\mathrm{tot}}}\int \mathrm{d}^2b\; b^2 \;\; \left[1 - \; e^{-\chi(\mathbf{b},s)}\,\right] . \tag{3.6}$$

### 3.1 Multi-parton scattering model

The preceding expressions are completely general and model-independent, but we now introduce an explicit model [8–11] to predict the form of the eikonal function, $\chi(\mathbf{b},s)$. First we assume that it can be decomposed into the sum of independent soft and hard parts,

$$\chi_{\mathrm{tot}}(\mathbf{b},s) = \chi_{\mathrm{QCD}}(\mathbf{b},s) + \chi_{\mathrm{soft}}(\mathbf{b},s)\,, \tag{3.7}$$

and start by considering the hard part. We consider a model in which partons are distributed across the face of the colliding hadrons with a spatial distribution that is independent of their longitudinal momentum. We assume that pairs of partons in the colliding



JHEP01(2009)065

hadrons scatter with independent probabilities, leading to the distribution of number of scatters at fixed impact parameter obeying Poisson statistics. We further assume that any hadron-hadron collision in which there is an elastic parton-parton collision above some cut-off $p_t^{\min}$ will lead to an inelastic hadronic final state. Finally, we require that the inclusive cross section for hadron-hadron collisions to produce partons above $p_t^{\min}$ be equal to the inclusive partonic cross section folded with standard inclusive parton distribution functions, as given by the factorization theorem. The result of this model is that the inelastic cross section is given by an expression identical to eq. 3.5, but with $\chi$ replaced by

$$\chi_{\rm QCD}(\mathbf{b}, s) = \frac{1}{2}\, A(\mathbf{b})\ \sigma^{\rm inc}_{\rm hard}(s; p_t^{\min})\,, \tag{3.8}$$

where $A(\mathbf{b})$ describes the overlap distribution of the partons in impact parameter space and $\sigma^{\rm inc}_{\rm hard}$ denotes the inclusive cross section above a transverse momentum cutoff $p_t > p_t^{\min}$, given by the perturbative result

$$\sigma^{\rm inc}_{\rm hard}(s; p_t^{\min}) = \sum_{ij} \int {\rm d}x_1\, {\rm d}x_2\ f_i(x_1)\, f_j(x_2) \int_{p_t^{\min}} {\rm d}p_t\, \frac{{\rm d}\hat{\sigma}_{ij}(x_i x_j s)}{{\rm d}p_t}, \tag{3.9}$$

where ${\rm d}\hat{\sigma}_{ij}(\hat{s})/{\rm d}p_t$ denotes the inclusive cross section for partons of types $i$ and $j$ and invariant-mass-squared $\hat{s}$ to produce jets of a given $p_t$.

We assume that the soft eikonal function has the same form,

$$\chi_{\rm soft}(\mathbf{b}, s) = \frac{1}{2}\, A_{\rm soft}(\mathbf{b})\ \sigma^{\rm inc}_{\rm soft}\,, \tag{3.10}$$

where $\sigma^{\rm inc}_{\rm soft}$ is the purely non-perturbative cross section below $p_t^{\min}$, which is a free parameter of the model. That is, we assume that soft scatters are the result of partonic interactions that are local in impact parameter.

The elastic slope parameter discussed above relates to bulk interactions of the proton. Thus it can be taken as directly constraining the matter distribution "seen" by soft scatters. Higher $p_t$ scatters might be expected to see a different matter distribution, for example they might probe denser "hot spots" within the proton. However, at present we take the simplest assumption for the perturbative part of the eikonal function, i.e. that the semi-hard scatters "see" the same matter distribution as the soft ones and therefore take $A(\mathbf{b}) \equiv A_{\rm soft}(\mathbf{b})$. This is clearly a simplifying assumption, but a reasonable one until proven otherwise.

It is worth mentioning that according to the definition in eq. 3.5, the inelastic cross section contains *all* inelastic processes, including diffractive dissociation. This is consistent with the calculation of the inclusive hard cross section, which is calculated from the conventional parton distribution functions, which describe the *inclusive* distribution of partons in a hadron whatever their source, i.e. whether the proton remains intact or not.

### 3.2 Overlap parameterization

The only remaining freedom in the eikonal model is the functional form of the overlap function $A(|\mathbf{b}| = b)$. $A(b)$ is the convolution of the individual spatial parton distributions

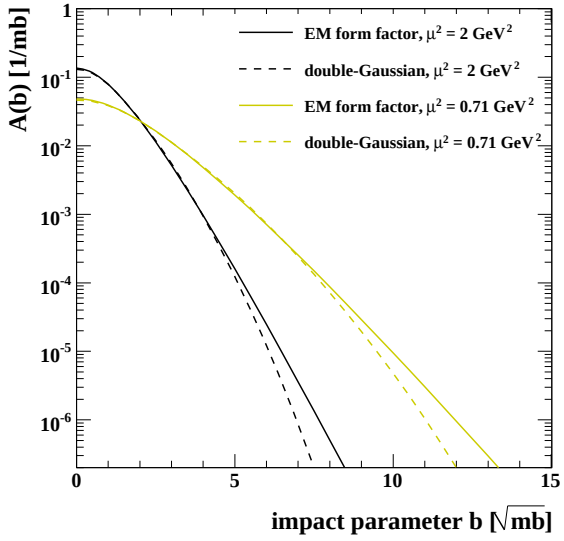


**Figure 2:** $A(b)$ for the two parameterizations.

of the colliding hadrons,

$$A(b) = \int d^2\mathbf{b}' \; G_{h_1}(|\mathbf{b}'|) \; G_{h_2}(|\mathbf{b} - \mathbf{b}'|) \, . \tag{3.11}$$

In refs. [9 – 11], $G(\mathbf{b})$ is taken to be proportional to the electromagnetic form factor,

$$G_{\bar{p}}(\mathbf{b}) = G_p(\mathbf{b}) = \int \frac{d^2\mathbf{k}}{(2\pi)^2} \; \frac{e^{i\mathbf{k}\cdot\mathbf{b}}}{(1 + \mathbf{k}^2/\mu^2)^2} \; . \tag{3.12}$$

$\mu$ is the only parameter and has the dimensions of an inverse radius. In $ep$ scattering its value was measured to be $\mu^2 = 0.71$ GeV$^2$. This is a loose constraint, since the distribution of partons may not necessarily coincide with the distribution of electromagnetic charge. Actually, using the results from the previous section, the CDF data on the total cross section ($\sigma_{\rm tot} = 81.8 \pm 2.3$ mb [13]) and the elastic slope ($B = 16.98 \pm 0.25$ GeV$^{-2}$ [19]) one can solve for the total inclusive cross section and for $\mu^2$, yielding $\mu^2 = 0.56 \pm 0.01$ GeV$^2$.

In order to investigate the dependence on the assumed shape of the matter distribution, we have compared our default results with those obtained with a double-Gaussian distribution, as chosen in refs. [21 – 23],

$$G(b) = \frac{1-\beta}{\pi r^2} \cdot \; e^{-\frac{b^2}{r^2}} \; + \frac{\beta}{\pi (k \cdot r)^2} \cdot \; e^{-\frac{b^2}{(k \cdot r)^2}} \; . \tag{3.13}$$

Here $\beta, k$ and $r$ are all free parameters, but we choose to fix $\beta$ and $k$ at values that are reasonably generic, but also close to the tuned values used in [21 – 23], with the relative strengths given by $\beta = 0.5$ and the relative widths by $k = 2$, and view $r$ as the only free parameter. The parameters $\mu^2$ and $r$ in the two models are arbitrary and should ultimately be fit to data. However, in order to have a like-for-like comparison, we choose to relate

them in such a way that the rms value of $G(b)$ is identical. That is, we describe the double-Gaussian also as being a function of $\mu^2$, with $r$ set via $b_{\rm rms}$. We illustrate the shapes of the two resulting overlap functions for two different values of $\mu^2$ in figure 2.

We find that for small values of $\mu^2$ ($\sim$ 1 GeV$^2$) the results of the two models are extremely similar, differing at most by $\pm 2$ %. For large values ($\sim$ 3 GeV$^2$) they differ more, the double Gaussian distribution giving a larger de-eikonalized cross section (see next section) by between 30 % with the standard Donnachie-Landshoff total cross section prediction at the LHC and 150 % with the soft+hard Pomeron prediction. While these lead to somewhat different predictions, in our final results they effectively correspond to a distortion of the $\mu^2$ axis. The effect on our final plots, figure 6, is small, since our consistency requirement is mainly active at small $\mu^2$.

### 3.3 Connection to the total cross section

For a given point in the parameter space $(p_t^{\rm min}, \mu^2)$ of our model, we are able to calculate $\chi_{\rm QCD}$ using eq. 3.8. The remaining uncertainty is in $\sigma_{\rm hard}^{\rm inc}(s; p_t^{\rm min})$, which depends on the PDF choice, the treatment of $\alpha_s$ etc. If we now choose a value for the non-perturbative cross section below $p_t^{\rm min}$, $\sigma_{\rm soft}^{\rm inc}$, we have the full eikonal function at hand and can calculate the total cross section from eq. 3.3.

We will, however, turn this argument around and use the value of the total cross section as input to fix the additional parameter in our non-perturbative part of the eikonal function ($\sigma_{\rm soft}^{\rm inc}$). For energies at which there are not yet measurements, we use the parameterizations of [3, 4] to give an indication of the likely range of the total cross section. We will extract the sum $\sigma_{\rm hard}^{\rm inc} + \sigma_{\rm soft}^{\rm inc} \equiv \sigma_{\rm de-eik}$ from eq. 3.3 and call this cross section the *de-eikonalized* cross section. That is, the de-eikonalized cross section is given by the solution to

$$\sigma_{\rm tot} = 2 \int {\rm d}^2 b \quad \left[ 1 - \; e^{-\frac{1}{2} A(\mathbf{b}) \sigma_{\rm de-eik}} \right] , \tag{3.14}$$

for a given value of $\mu^2$ and a given value of the total cross section, $\sigma_{\rm tot}$. Clearly, $\sigma_{\rm de-eik}$ is a function only of these two quantities. Since $\sigma_{\rm hard}^{\rm inc}$ is $p_t^{\rm min}$-dependent, this implies that the value of $\sigma_{\rm soft}^{\rm inc}$ we extract by this procedure is also $p_t^{\rm min}$-dependent ($p_t^{\rm min}$ is a *matching* scale between the two sub-process cross sections and the sum of the two is independent of it).

In figure 3 we plot the de-eikonalized cross sections for the three different total cross section extrapolations as a function of the centre-of-mass energy. Furthermore we show the value of $\sigma_{\rm hard}^{\rm inc}$ using different cutoffs. $\sigma_{\rm soft}^{\rm inc}$ is now given by the difference of these curves. If we interpret $\sigma_{\rm soft}^{\rm inc}$ as a physical cross section (the inclusive cross section for two partons to undergo a non-perturbative soft scattering), it cannot be negative. Thus the implication is that whenever the inclusive hard cross section is larger than the de-eikonalized one, the model is inconsistent. We will investigate this behaviour in more detail in section 4.1.

From the plots in figure 3 the values for $\sigma_{\rm soft}^{\rm inc}$ can in principle be read off. However, due to the logarithmic scale it is not easy to see what is implied for the energy dependence of the soft cross section. Therefore, for selected points in parameter space, $\sigma_{\rm soft}^{\rm inc}$ is shown separately in figure 4. Note that where the inclusive hard cross section line for $p_t^{\rm min} = 3.0\,{\rm GeV}$ crosses and re-crosses the total cross-section extrapolation in the top left plot of

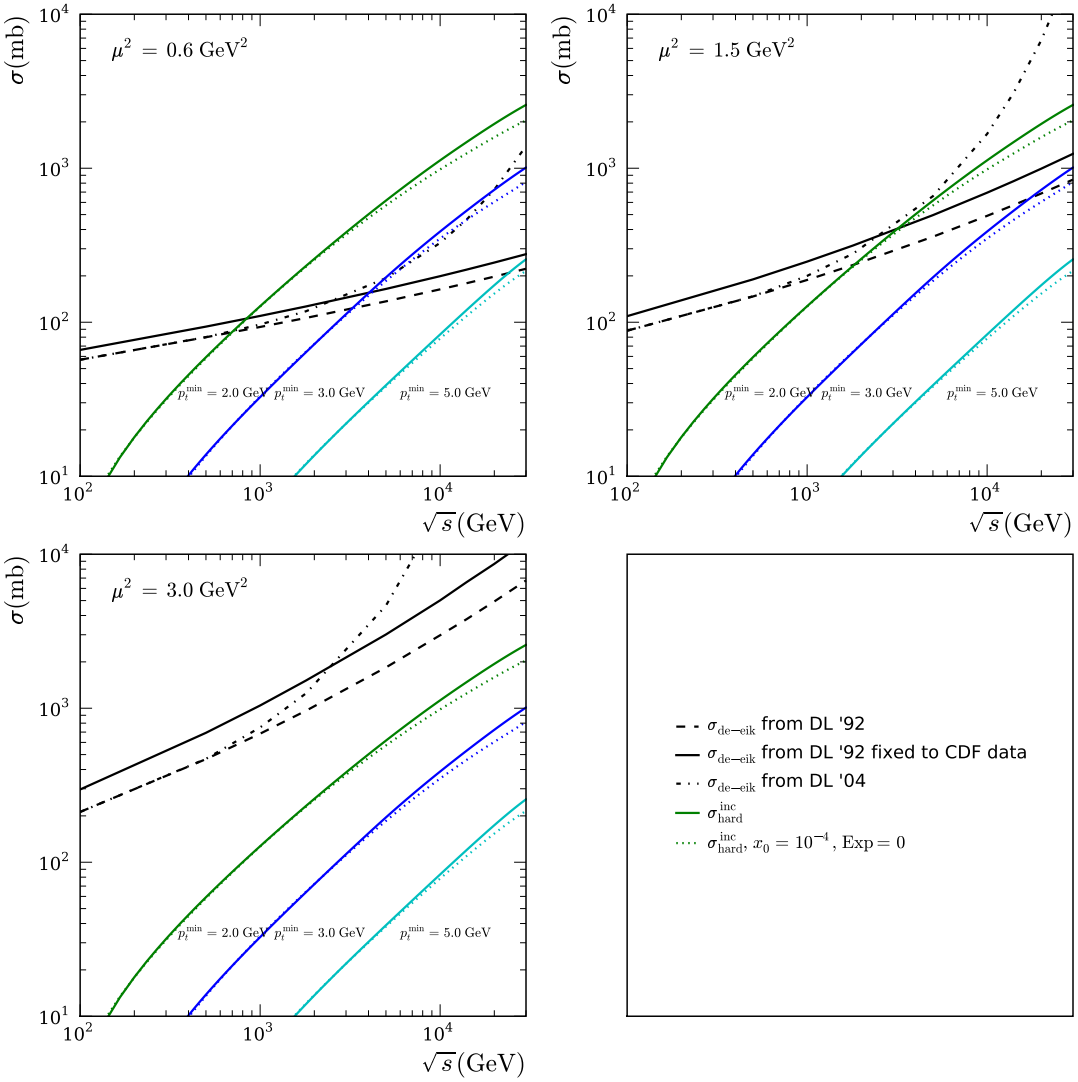


**Figure 3:** Cross sections in millibarn as a function of the centre-of-mass energy in GeV. The three different plots vary the value of $\mu^2$ from 0.6 to 3 GeV$^2$. The black curves show de-eikonalized total cross sections. We use the total cross section parameterization of ref. [3] for the dashed curves. The solid curves use the same exponent, but the normalization is rescaled to fit the total cross section measurement of CDF. The dotted curve uses the parameterization of ref. [4]. The coloured solid curves show $\sigma_{\text{hard}}^{\text{inc}}$ for different values of $p_t^{\text{min}}$. The coloured dash-dotted curves incorporate the simple small-$x$ deviations discussed in section 3.4

figure 3, the soft cross section in the top left plot of figure 4 first becomes negative and then positive again. The dependence of $\sigma_{\text{soft}}^{\text{inc}}$ on the centre-of-mass energy reveals two main points: First, it is noticeable that one observes a more-or-less constant behaviour with increasing energy only in a limited range of our parameter space. This behaviour is mainly present for lower values of $\mu^2$. Second, for the most extreme total cross section prediction, $\sigma_{\text{hard}}^{\text{inc}}$ is *never* sufficient to explain the strong rise with energy. There, essentially all parameter choices require a strongly rising *soft* cross section, in addition to the expected



JHEP01(2009)065

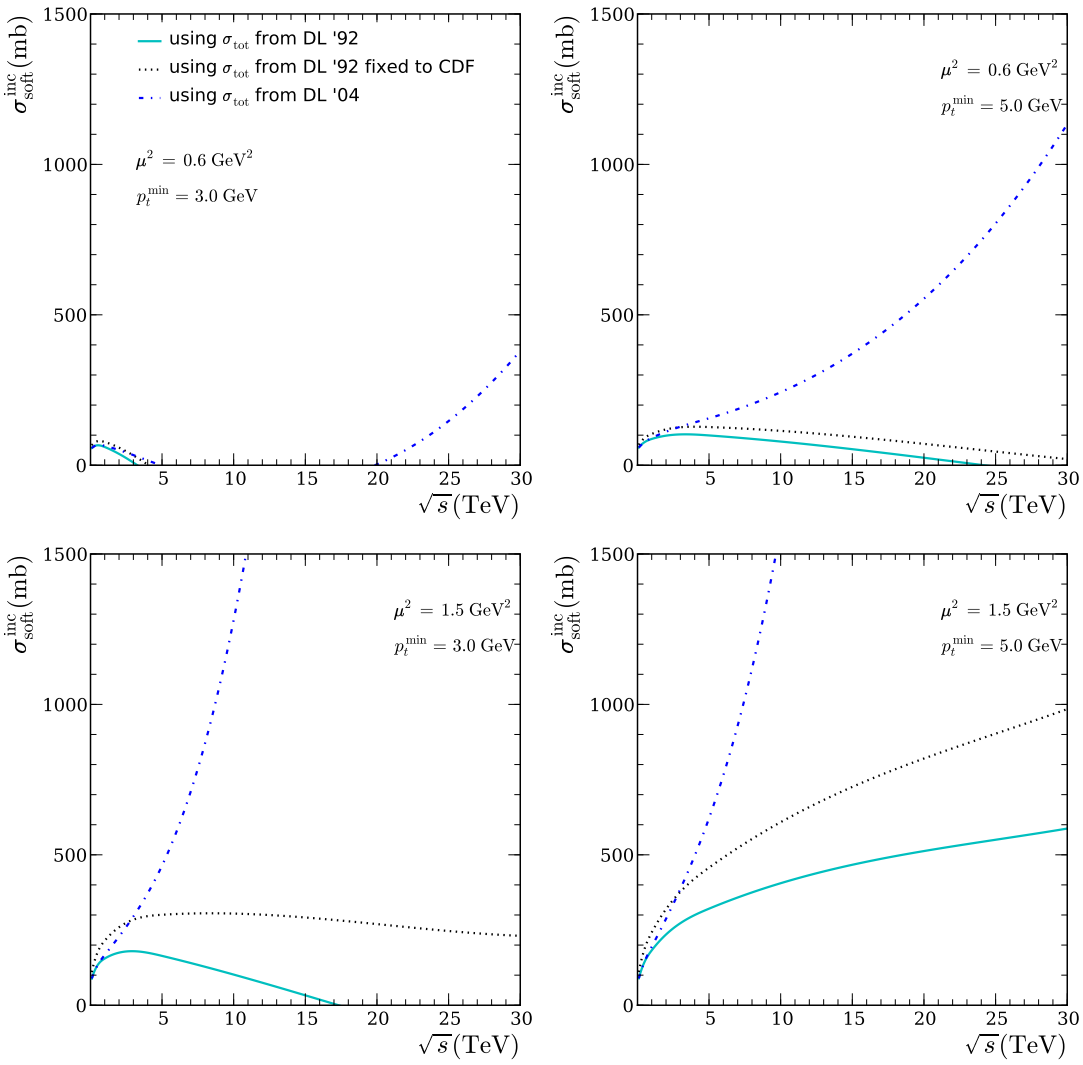


**Figure 4:** $\sigma_{\rm soft}^{\rm inc}$ for four different points in parameter space. As explained in the text, the extracted value of $\sigma_{\rm soft}^{\rm inc}$ depends on the values of $\sigma_{\rm tot}$, $\mu^2$ and (through the fact that $\sigma_{\rm soft}^{\rm inc} = \sigma_{\rm de-eik} - \sigma_{\rm hard}^{\rm inc}$) $p_t^{\rm min}$. Each panel shows a different pair of $\mu^2$ and $p_t^{\rm min}$ parameters, while the three different curves in each use the three parameterizations for the total cross section as a function of energy.

strong rise in the hard cross section. This is, at the very least, counter-intuitive, and one might conclude that, within our model, the rise of the cross section in parametrization (2.3) is too extreme.

### 3.4 Parton saturation physics

The main motivation for allowing multiparton scatterings is the rise of the inclusive cross section, for fixed $p_t^{\rm min}$, with increasing centre-of-mass energy. Multiparton scattering provides a mechanism to allow this quantity to exceed the total cross section. Eikonal models that incorporate this fact unitarize the inclusive cross section. There is however a second source of unitarization, the physics of parton saturation, which is a competing effect. To



JHEP01(2009)065

estimate the influence on our studies, we have used a simple modification of the PDFs recently introduced [24] into Herwig++ to mimic parton saturation effects for any PDF. The modification replaces $xf(x)$ below $x_0$ by

$$xf(x) \to \left(\frac{x}{x_0}\right)^{\mathrm{Exp}} x_0 f(x_0) \quad \forall\, x < x_0\,, \tag{3.15}$$

where **X0** and **Exp** are changeable parameters. HERA data indicate that saturation is unlikely to be a strong effect above $x \approx 10^{-4}$. Therefore, the strongest reasonable influence from this effect is obtained by setting $x_0 = 10^{-4}, \mathrm{Exp} = 0$. The results are shown in figure 3, where the effect is visible, but small, at LHC energies.

## 4. Parameter space constraints from data

In discussing the de-eikonalized cross section, we noted that for some parameter values the hard partonic cross section exceeds it. This implies in our model that the soft cross section should be negative. We take this as an inconsistency that would, for a given measured $\sigma_{\mathrm{tot}}$ at the LHC, rule out such parameter space points. In this section we discuss the extent to which the space of parameter values can be limited by this and other constraints.

### 4.1 Consistency

The parameter space in $\mu^2$ and $p_t^{\mathrm{min}}$ is shown in figure 5 for the Tevatron, and figure 6 for the LHC.

The horizontal band shows the range of $\mu^2$ values allowed for a given value of the elastic slope in conjunction with the indicated $\sigma_{\mathrm{tot}}$. For Tevatron energies, both $B$ and $\sigma_{\mathrm{tot}}$ are chosen according to the CDF measurement from refs. [13] and [19] respectively.

Our expectations on the value of the elastic slope at LHC energies simply reflect the range of predictions that the models of [3, 4, 14, 15] give, as discussed in section 2. For the value of $\sigma_{\mathrm{tot}}$ at the LHC we show a range of possible values motivated by these parameterizations.

For a particular value of $\sigma_{\mathrm{tot}}$ (or for a given range of possible values at the LHC), we are able to extract constraints on the allowed parameters, by simply requiring a sensible performance of the eikonal model. The most basic requirement, which was just mentioned, is that the non-perturbative cross section that is needed to match the total cross-section prediction is positive. A negative value means that the model cannot be applied and therefore this requirement puts a stringent limit on the allowed values of $\mu^2$ and $p_t^{\mathrm{min}}$. This limit will depend on the value of $\sigma_{\mathrm{hard}}^{\mathrm{inc}}$, which is not a stable prediction itself. We therefore calculate this limit with several variations. We use three different PDF sets [25 – 27], vary the running of $\alpha_s$ from 1-loop, which is the default in Herwig++ to 2-loop and finally apply the modifications to the PDF's described in section 3.4. The solid lines in figures 5 and 6 show these limits, where the entire range below the curves is excluded. The limits impose a minimal $\mu^2$ for any given value of $p_t^{\mathrm{min}}$. Points on that line are parameter sets where $\sigma_{\mathrm{soft}}^{\mathrm{inc}} = 0$ mb.



JHEP01(2009)065

Another, weaker, consistency constraint we apply is related to the simulation of the final state of these collisions. We observe that when we embed them into the full simulation of Herwig++, including backward evolution of the initial state, each collision consumes, on average, about a tenth of the available total energy, so that the approximation that individual hard scatters are independent must break down, at least due to energy conservation, when there are more than about ten of them. We therefore indicate on figure 6 the points in parameter space where the average multiplicity of scatters above $p_t^{\min}$ reaches 10. This is certainly not a stringent limit but a sensible parameter choice most likely avoids this region.

The classic CDF analysis of the distribution in azimuth of the mean charged multiplicity and scalar $p_t$ sum as a function of the transverse momentum of the leading jet [6] also provides constraints on the model as embedded in Herwig++. Reference [11] described the implementation of multiparton scattering into Herwig++ (i.e. the simulation of the final state corresponding to $\sigma_{\rm hard}^{\rm inc}$) and made a two-parameter fit ($\mu^2$ and $p_t^{\min}$) to these data. Since Herwig++ does not yet include a simulation of the final state corresponding to $\sigma_{\rm soft}^{\rm inc}$, we do not take the results of this fit as a strong constraint on the parameter space, but an indication of the effect such a tuning could have once a complete description is available. The result is that, although one obtains a best fit with the values $\mu^2 = 1.5$ GeV$^2$, $p_t^{\min} = 3.4$ GeV, the best-fit values of the parameters are strongly correlated, with the $\chi^2$ function having a long, thin, rather flat valley running from ($p_t^{\min} = 2.5$ GeV, $\mu^2 \sim 0.7$ GeV$^2$) to ($p_t^{\min} = 4.5$ GeV, $\mu^2 \sim 2.5$ GeV$^2$), and beyond. For any given value of $p_t^{\min}$ in this range one can find a $\mu^2$ value that gives a good description of these data.

Combining these constraints at the Tevatron, a small allowed region remains around $p_t^{\min} = 2.3$ GeV and $\mu^2 = 0.6$ GeV$^2$.

At the LHC, this region would be ruled out for all the values of $\sigma_{\rm tot}$ we have considered. Note that if the LHC measurement were as high a 164 mb, this would on its own imply an energy-dependent $\mu^2$, in contradiction with our initial assumptions.

In the next section we discuss different ways in which the assumptions of the model might be modified to account for this potential inconsistency.

### 4.2 Extensions to the model

Some authors have suggested, within multiparton scattering models, that the parameters of the model, analogous to our $\mu^2$ and $p_t^{\min}$, should be energy dependent. In this section we briefly discuss the arguments for these models.

In [28] a simple model of the spatial/momentum structure of a hadron was constructed from which it was argued that the colour screening length decreases slowly with increasing energy. This translates into a $p_t^{\min}$ that increases slowly with energy, for which they estimated $p_t^{\min} \sim s^{\epsilon}$ with $\epsilon$ in the range 0.025 to 0.08. The actual value used in refs. [21 – 23] is 0.08, leading to a 35% increase in $p_t^{\min}$ from the Tevatron to the LHC.

In [29, 30] a multiparton model was constructed that is very similar to ours at low energy, with an impact parameter distribution of partons given by the electromagnetic form factor. However, soft gluon effects were estimated and summed to all orders, to give



JHEP01(2009)065

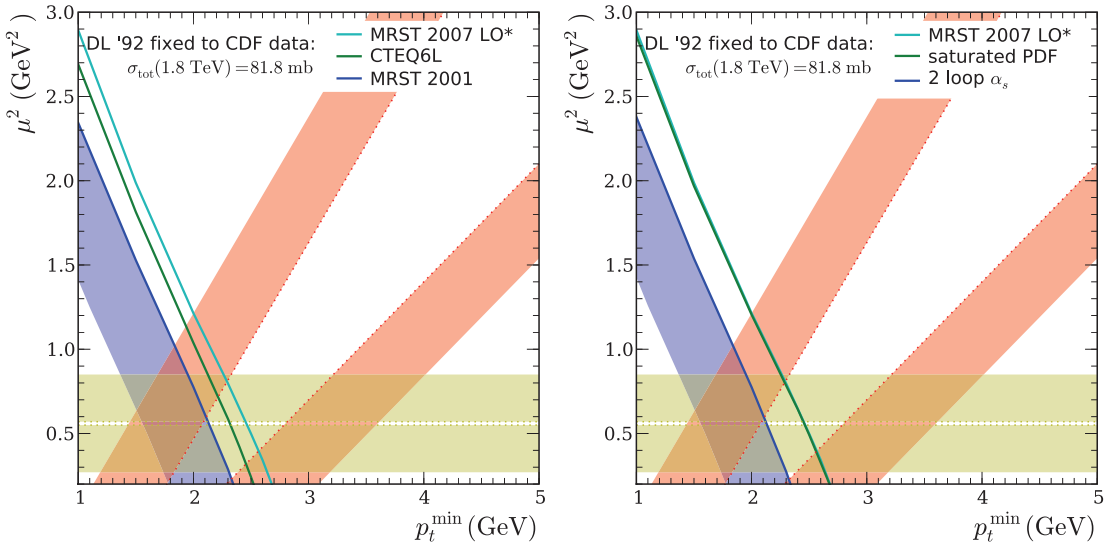


**Figure 5:** The parameter space of the eikonal model at Tevatron energies. The solid curve imposes a minimum allowed value of $\mu^2$, for a given value of $p_t^{\rm min}$ by requiring a positive value of $\sigma_{\rm soft}^{\rm inc}$. The horizontal lines correspond to the measurement of $B = 16.98 \pm 0.25$ GeV$^{-2}$ from CDF [13]. The excluded regions are shaded. The dashed lines indicate the region of preferred parameter values for a fit to Tevatron final-state data from ref. [11], which used the MRST2001 PDF set. The left plot shows the PDF uncertainty by varying the PDF set. The right plot shows the uncertainty that is implied by using 2-loop $\alpha_s$ running and using the saturation modifications.

a mean parton-parton separation, $b_{\rm rms}$, that falls with energy, quickly at first, but then saturating: the value at 1 TeV is about a factor of two smaller than at low energy, while the value at 14 TeV is only about 10% smaller still. In terms of our simple model in which the matter distribution always has the form factor form and is parameterized by $\mu^2$, $\langle b^2 \rangle \propto 1/\mu^2$ and this corresponds to $\mu^2 \sim 2.8$ GeV$^2$ at the Tevatron and $\sim 3.4$ GeV$^2$ at the LHC. Not only would this introduce an energy dependence in $\mu^2$, but the values imply a different $\mu^2$ for hard partonic interactions than that derived from the measured elastic slope parameter, a point that we will return to below.

Note that both these sources of energy dependence would act in the right direction to evade the potential consistency constraints at the LHC. Allowing $p_t^{\rm min}$ and/or $\mu^2$ to increase with energy would move the model towards the allowed region in figure 6.

The CDF collaboration have published measurements of the double-parton scattering cross section [31, 32]. As pointed out in ref. [33] the quantity called $\sigma_{\rm eff}$ there is not the effective cross section as it is usually defined,

$$\sigma_{\rm eff} = \frac{1}{\int d^2\mathbf{b} \big(A(b)\big)^2}, \tag{4.1}$$

but is related to the latter by a small correction. Using the value of this correction estimated in ref. [34], we obtain $\sigma_{\rm eff} \sim 11.5 \pm 2$ mb. In our form factor model, this corresponds to $\mu^2 \sim 3.0 \pm 0.5$ GeV$^2$. It is interesting to note that this value is close to the one predicted by the analysis of refs. [29, 30] mentioned earlier. Again, this value is inconsistent with



JHEP01(2009)065

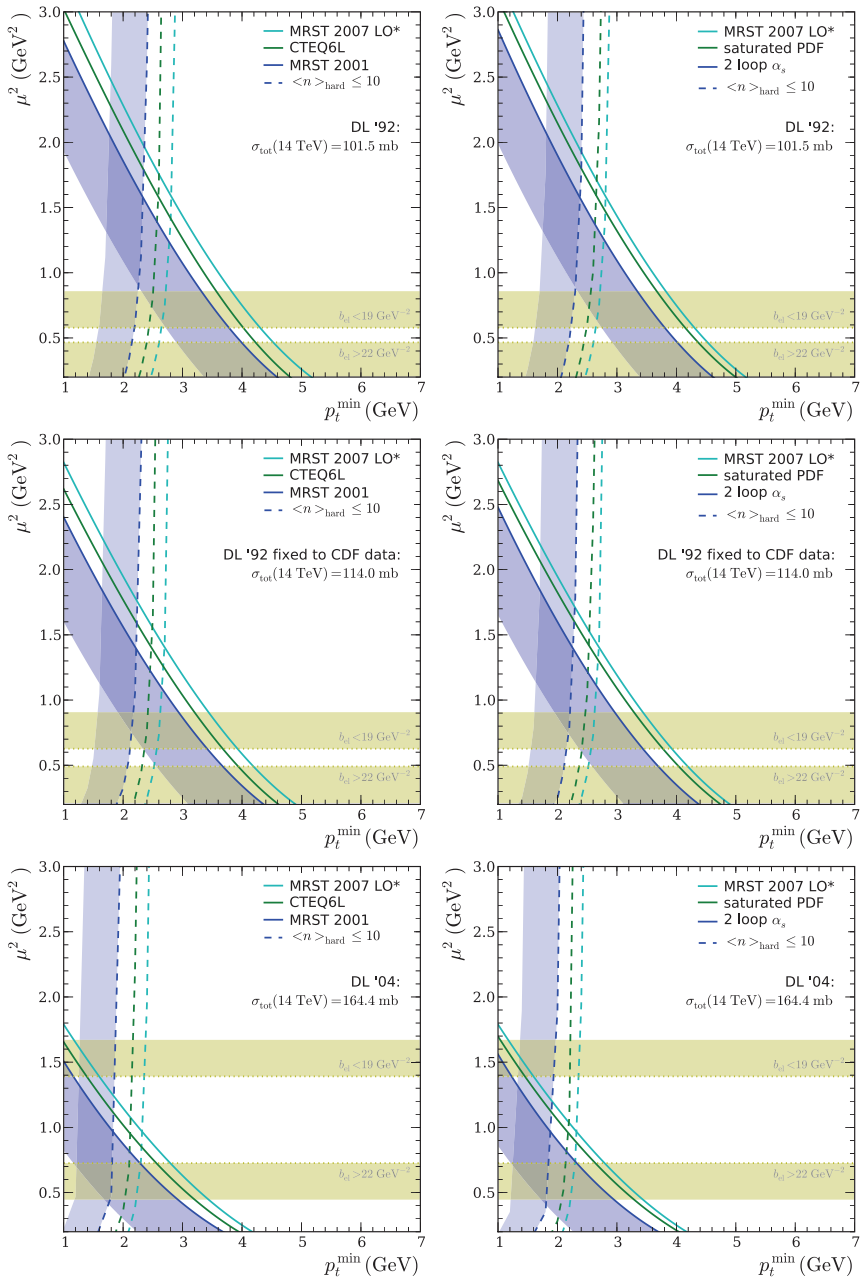


**Figure 6:** The parameter space of the eikonal model and three constraints. The first one drawn as solid curve imposes a minimum allowed value of $\mu^2$, for a given value of $p_t^{\min}$ by requiring a positive value of $\sigma_{\rm soft}^{\rm inc}$. The second one, in dashed lines is deduced from an upper limit of the average number of additional semi-hard scatters in a typical minimum bias event. The excluded regions are shaded. The third constraint comes from the expected range of values for the elastic slope $B$. From top to bottom we calculate these constraints for the three different total cross sections at LHC, discussed in section 2, always with the same range of $B = 19 - 22$ GeV$^{-2}$. Finally the left column shows the PDF uncertainty by varying the PDF set. The right column shows the uncertainty that is implied by using 2-loop $\alpha_s$ running and using the saturation modifications.

JHEP01(2009)065

the assumption that the hard scatters "see" a form factor matter distribution derived from the elastic slope parameter. Recall from our earlier discussion that we do not expect significant qualitative differences for other models of the matter distribution in the proton, merely some distortions of the parameter-space plane.

Improved analyses of these and other observables are under way and, once completed, in particular with a simulation of the final state of $\sigma_{\rm soft}^{\rm inc}$, will provide strong constraints on the values of the parameters $\mu^2$ and $p_t^{\rm min}$ in our model.

## 5. Conclusions

The connections between our underlying event model and the total proton-proton cross-section have been discussed. Requiring consistency of the model up to LHC energies imposes constraints on the allowed parameter values, for a given range of possible measurements of $\sigma_{\rm tot}$ at the LHC. Our main result is summarized in figure 6, which shows these constraints for various values of the total cross section at the LHC and various inputs to the perturbative cross section calculation. Taking the Tevatron data together with the wide range of possible values of $\sigma_{\rm tot}$ considered at LHC, no allowed set of parameters ($\mu^2$, $p_t^{\rm min}$) remains for our simple model.

This would imply that soft and hard scatters see different matter distributions as a function of impact parameter and/or that the parameters of our model are energy dependent. The measurement of double-parton scattering at the Tevatron supports the idea that hard scatters see a more dense matter distribution than is implied by the $t$-slope of the elastic cross section. Various phenomenological models also predict such effects.

With steadily improving data from the Tevatron, more detailed phenomenological analyses being performed and the prospect of data from the LHC, there is a real hope that the various simplifying assumptions that go into our model will be tested to the limit and we will discover where, if anywhere, more detailed understanding of the dynamics of underlying event physics is needed. The biggest unknown in our analysis is the total cross section at the LHC. With even a first imprecise measurement of this cross section, we could strengthen our parameter space analysis considerably.

## Acknowledgments

We are grateful for discussions with Stefan Gieseke and Jeff Forshaw. This work was supported in part by the European Union Marie Curie Research Training Network MCnet under contract MRTN-CT-2006-035606. MB was supported by the Landesgraduiertenförderung Baden-Württemberg.

## References

[1] ZEUS collaboration, S. Chekanov et al., *Measurement of the neutral current cross section and $F2$ structure function for deep inelastic $e^+p$ scattering at HERA*, *Eur. Phys. J.* **C 21** (2001) 443 [hep-ex/0105090].

[2] H1 collaboration, C. Adloff et al., *Deep-inelastic inclusive ep scattering at low x and a determination of $\alpha_s$*, *Eur. Phys. J.* **C 21** (2001) 33 [hep-ex/0012053].

[3] A. Donnachie and P.V. Landshoff, *Total cross-sections*, *Phys. Lett.* **B 296** (1992) 227 [hep-ph/9209205].

[4] A. Donnachie and P.V. Landshoff, *Does the hard Pomeron obey Regge factorisation?*, *Phys. Lett.* **B 595** (2004) 393 [hep-ph/0402081].

[5] T. Sjöstrand and M. van Zijl, *A multiple interaction model for the event structure in hadron collisions*, *Phys. Rev.* **D 36** (1987) 2019.

[6] CDF collaboration, A.A. Affolder et al., *Charged jet evolution and the underlying event in $p\bar{p}$ collisions at* 1.8 *TeV*, *Phys. Rev.* **D 65** (2002) 092002.

[7] ZEUS collaboration, S. Chekanov et al., *Three- and four-jet final states in photoproduction at HERA*, *Nucl. Phys.* **B 792** (2008) 1 [arXiv:0707.3749].

[8] L. Durand and H. Pi, *Semihard QCD and high-energy pp and $\bar{p}p$ scattering*, *Phys. Rev.* **D 40** (1989) 1436.

[9] J.M. Butterworth, J.R. Forshaw and M.H. Seymour, *Multiparton interactions in photoproduction at HERA*, *Z. Physik* **C 72** (1996) 637 [hep-ph/9601371].

[10] I. Borozan and M.H. Seymour, *An eikonal model for multiparticle production in hadron hadron interactions*, *JHEP* **09** (2002) 015 [hep-ph/0207283].

[11] M. Bahr, S. Gieseke and M.H. Seymour, *Simulation of multiple partonic interactions in HERWIG++*, *JHEP* **07** (2008) 076 [arXiv:0803.3633].

[12] M. Bahr et al., *HERWIG++ physics and manual*, *Eur. Phys. J.* **C 58** (2008) 639 [arXiv:0803.0883].

[13] CDF collaboration, F. Abe et al., *Measurement of the $\bar{p}p$ total cross-section at $\sqrt{s} = 546$ GeV and* 1800 *GeV*, *Phys. Rev.* **D 50** (1994) 5550.

[14] V.A. Khoze, A.D. Martin and M.G. Ryskin, *Soft diffraction and the elastic slope at Tevatron and LHC energies: a multi-Pomeron approach*, *Eur. Phys. J.* **C 18** (2000) 167 [hep-ph/0007359].

[15] E. Gotsman, E. Levin and U. Maor, *A soft interaction model at ultra high energies: amplitudes, cross sections and survival probabilities*, arXiv:0708.1506.

[16] M.G. Ryskin, A.D. Martin and V.A. Khoze, *Soft diffraction at the LHC: a partonic interpretation*, *Eur. Phys. J.* **C 54** (2008) 199 [arXiv:0710.2494].

[17] E. Gotsman, E. Levin, U. Maor and J.S. Miller, *A QCD motivated model for soft interactions at high energies*, *Eur. Phys. J.* **C 57** (2008) 689 [arXiv:0805.2799].

[18] TOTEM collaboration, M. Deile et al., *Diffraction and total cross-section at the Tevatron and the LHC*, hep-ex/0602021.

[19] CDF collaboration, F. Abe et al., *Measurement of small angle $\bar{p}p$ elastic scattering at $\sqrt{s} = 546$ GeV and* 1800 *GeV*, *Phys. Rev.* **D 50** (1994) 5518.

[20] M.M. Block and R.N. Cahn, *High-energy $p\bar{p}$ and pp forward elastic scattering and total cross-sections*, *Rev. Mod. Phys.* **57** (1985) 563.

JHEP01(2009)065

[21] T. Sjöstrand and P.Z. Skands, *Multiple interactions and the structure of beam remnants*, *JHEP* **03** (2004) 053 [hep-ph/0402078].

[22] T. Sjöstrand, S. Mrenna and P. Skands, *PYTHIA* 6.4 *physics and manual*, *JHEP* **05** (2006) 026 [hep-ph/0603175].

[23] T. Sjöstrand, S. Mrenna and P. Skands, *A brief introduction to PYTHIA* 8.1, *Comput. Phys. Commun.* **178** (2008) 852 [arXiv:0710.3820].

[24] M. Bähr et al., *HERWIG++* 2.2 *release note*, arXiv:0804.3053.

[25] A.D. Martin, R.G. Roberts, W.J. Stirling and R.S. Thorne, *MRST*2001*: partons and* $\alpha_s$ *from precise deep inelastic scattering and Tevatron jet data*, *Eur. Phys. J.* **C 23** (2002) 73 [hep-ph/0110215].

[26] J. Pumplin et al., *New generation of parton distributions with uncertainties from global QCD analysis*, *JHEP* **07** (2002) 012 [hep-ph/0201195].

[27] A. Sherstnev and R.S. Thorne, *Parton distributions for LO generators*, *Eur. Phys. J.* **C 55** (2008) 553 [arXiv:0711.2473].

[28] J. Dischler and T. Sjöstrand, *A toy model of colour screening in the proton*, *Eur. Phys. J. direct* **C3** (2001) 2 [hep-ph/0011282].

[29] R.M. Godbole, A. Grau, G. Pancheri and Y.N. Srivastava, *Soft gluon radiation and energy dependence of total hadronic cross-sections*, *Phys. Rev.* **D 72** (2005) 076001 [hep-ph/0408355].

[30] A. Achilli et al., *Total cross-section and rapidity gap survival probability at the LHC through an eikonal with soft gluon resummation*, *Phys. Lett.* **B 659** (2008) 137 [arXiv:0708.3626].

[31] CDF collaboration, F. Abe et al., *Measurement of double parton scattering in* $\bar{p}p$ *collisions at* $\sqrt{s} = 1.8$ *TeV*, *Phys. Rev. Lett.* **79** (1997) 584.

[32] CDF collaboration, F. Abe et al., *Double parton scattering in* $\bar{p}p$ *collisions at* $\sqrt{s} = 1.8$ *TeV*, *Phys. Rev.* **D 56** (1997) 3811.

[33] D. Treleani, *Double parton scattering, diffraction and effective cross section*, *Phys. Rev.* **D 76** (2007) 076006 [arXiv:0708.2603].

[34] M. Bähr and M.H. Seymour, in preparation.

JHEP01(2009)065